Charmed Hadron Spectroscopy at FOCUS

Robert K. Kutschke
Fermi National Accelerator Laboratory
(Representing the FOCUS[1] Collaboration)

May 29, 2001

Abstract

The FOCUS experiment at Fermilab is a high statistics charm photoproduction experiment, which acquired data in 1996 and 1997. This report presents preliminary measurements of the masses and widths of the of the P-wave charmed mesons, including the first observation of the decay mode $D^*_{s2} \to D^+ K^0_S$. It also presents a measurement of the $\Sigma_c^{++} - \Sigma_c^0$ isospin mass splitting and preliminary measurements of the natural widths of these states. It concludes with preliminary measurements of the masses and widths of the Σ_c^+, Σ_c^{*++}, Σ_c^{*0}.

1 The FOCUS Detector

The FOCUS detector[2] was designed to make precision measurements of charmed hadrons produced by the interaction of a high energy photon with a beryllium oxide target. The detector was located in the Fermilab the wideband photon beam and the data presented here were taken during the 1996-97 fixed target run.

The photon beam was created by the bremsstrahlung of electron and positron beams; typically the endpoint of the photon energy spectrum was about 300 GeV. This beam was incident on a segmented beryllium oxide target, and the resulting charmed hadrons were detected using the FOCUS detector, an upgraded version of the Fermilab E687 Spectrometer[3]. One of the upgrades was to replace the bulk target with a segmented target and to add silicon strip detectors interspersed among the target planes. Other upgraded systems include the EM calorimeter and the Čerenkov, muon and data acquisition systems. FOCUS has more than ten times the reconstructed charm yield of its predecessor. One figure of merit is the yield of the so-called Golden Modes, $D^0 \to K^-\pi^+$, $D^0 \to K^-\pi^+\pi^+\pi^-$ and $D^+ \to K^-\pi^+\pi^+$: FOCUS has reconstructed more than one million Golden Mode candidates, with a signal to background ratio (S/B)

of about 0.6. Significantly better S/B can be obtained at the cost of some signal efficiency.

The FOCUS charged particle tracking system consists of 4 planes of silicon strip detectors, which are interspersed among the target planes, a 12 plane silicon strip system, immediately downstream of the targets, and 5 stations of multiwire proportional chambers (MWPC), located further downstream. The momentum of a charged particle is determined by using the MWPC's to measure the bend of the trajectory in a pair of oppositely polarized dipole magnets. Three multicell threshold Čerenkov counters are used to discriminate among electrons, pions, kaons and protons.

Photons are detected using two EM calorimeter technologies. Photons in the central region are detected using the inner EM calorimeter, which is built from lead glass blocks. Photons at wider angles are detected using the outer EM calorimeter, a sampling calorimeter consisting of alternating layers of lead and plastic scintillator.

2 Candidate Driven Vertexing

All of the analyses discussed in this report use candidate driven vertexing, which will be described using the example of $D^+ \to K^-\pi^+\pi^+$.[1] The first step is to apply track quality and particle ID cuts to all measured tracks in an event. Details of the particle ID algorithm can be found in ref.[4]. Using the tracks passing these cuts, all possible $K^-\pi^+\pi^+$ combinations are made. For each combination the three tracks are fitted to the hypothesis that they come from a common vertex and only candidates with a good confidence level are retained. It is also required that the invariant mass of the combination be close to the PDG value of the D^+ mass. Each surviving combination is used to seed a search for a primary vertex: one treats the $K^-\pi^+\pi^+$ system as just another track and searches for other tracks which intersect its trajectory. This process defines two vertices, the primary vertex at which the D^+ was produced, and a displaced secondary vertex at which it decayed. The minimal requirement is that the primary vertex be formed from the $K^-\pi^+\pi^+$ trajectory plus at least one other charged track, but some of the analyses presented here require at least two other charged tracks. It is also required that the decay length, L, be large compared to is error, σ_L. In typical FOCUS analyses the requirements on L/σ_L range from a loose cut of $L/\sigma_L > 3$ to a tight cut of $L/\sigma_L > 10$ or more. Two other isolation requirements are typically imposed: that none of the D^+ daughter tracks are consistent with passing through the primary vertex and that no other tracks in the event are consistent with passing through the $K^-\pi^+\pi^+$ decay vertex. If an event contains more than one $K^-\pi^+\pi^+$ combination which passes all of the above cuts, both are accepted as D^+ candidates and the primary vertex finding is done separately for each candidate. To search for excited charmed states,

[1] Any reference in this paper to a specific charge state also implies a reference to the charge conjugate state.

each D^+ candidate in an event is combined with all other tracks in the event that are consistent with coming from the primary vertex.

3 P-wave Charmed Meson Analysis

The predicted P-wave charmed meson sector consists of 12 states, four in each of the D^+, D^0 and D_s sectors. The gross structure of this sector is easily understood by exploiting the idea of Heavy Quark Symmetry, which holds exactly in the limit that the mass of the charmed quark, m_c, satisfies $m_c >> \Lambda_{\rm QCD}$. The known mass of the charmed quark, around 1.5 GeV/c^2, is heavy enough that the HQS limit provides a very good description of P-wave charm sector. HQS predicts that, within each flavor sector, the four states will appear as a narrow doublet, in which the two states have widths of order 20 MeV, and a broad doublet, in which the two states have widths of at least 100 MeV, perhaps much more. The one exception to this pattern is the $D_{s1}(2536)$, one of the narrow states, which is so close to threshold that its width is very small, less than 2.3 MeV at the 90% CL. An excellent review on P-wave charmed mesons, including references to much of the theory, can be found in ref.[5].

All six of the predicted narrow states have been observed. While there is some evidence for some of the six broad states, none are firmly established. FOCUS has observed the 5 of the 6 narrow P-wave charmed mesons: $D_2^{*0}(2460)$, $D_2^{*+}(2460)$, $D_1^0(2420)$, $D_{s1}^+(2536)$ and $D_{s2}^{*+}(2573)$. Preliminary results from this work are summarized here.

3.1 P-wave Charmed-strange Mesons

The D_{s2}^* meson has been observed in only one decay mode, D^0K^+. The other allowed decay modes are $D^+K_S^0$, $D^{*0}K^+$ and $D^{*+}K_S^0$. To search for this state, the following decay chains were considered, $D_{s2} \to D^0K^+$, followed by $D^0 \to K^-\pi^+$ or $D^0 \to K^-\pi^+\pi^+\pi^-$. The D^0 candidates were reconstructed using the candidate driven approach described in section 2. Each D^0 candidate was combined with each K^+ candidate, in the same event, which was consistent with coming from the primary vertex. For each D^0K^+ combination the mass difference Δ_{s0} was computed, where,

$$\Delta_{s0} = M((K^-\pi^+[\pi^+\pi^-])K^+) - M(K^-\pi^+[\pi^+\pi^-]). \qquad (1)$$

The distribution of Δ_{s0} for all combinations which pass the analysis cuts is shown as the data points in fig. 1a). The prominent structure near a mass difference of 0.7 GeV/c^2 corresponds to the D_{s2} while the narrow structure near a mass difference of 0.525 GeV/c^2 arises from a feed-down process, $D_{s1} \to D^{*0}K^+$ followed by $D^{*0} \to D^0\pi^0$ or $D^{*0} \to D^0\gamma$. Two properties conspire to give the feed-down peak its narrow width. First, the natural width of the D_{s1} is less than 2.3 MeV at the 90% CL. Second, the Q values of the D^* decays are small; therefore the kinematic broadening due to missing the neutral is also

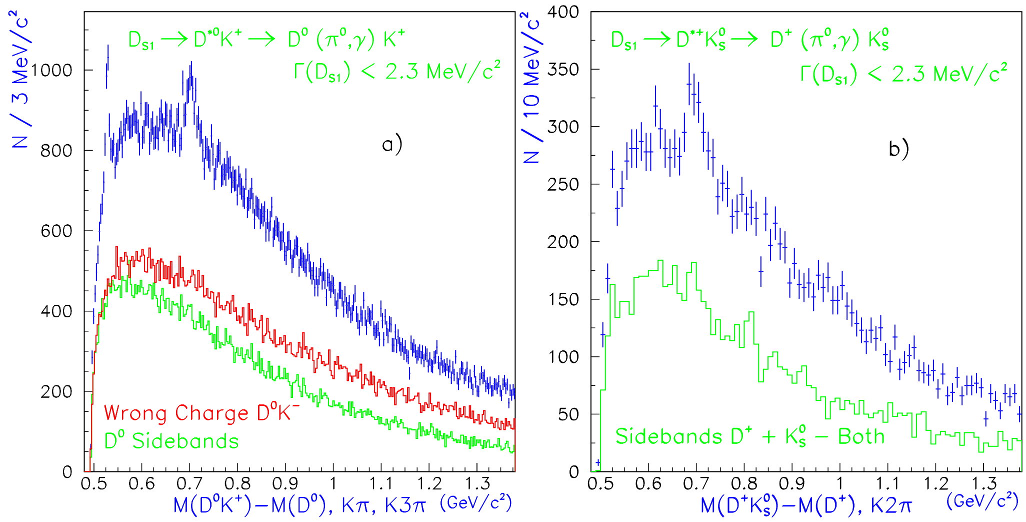

Figure 1: *Mass difference distributions for a) D^0K^+ and b) $D^+K^0_S$ combinations. The superimposed histograms are various background estimators which are described in the text. The structures in the data are also described in the text.*

small. This sort of feed-down will be present in most plots shown in the P-wave charm section of this report. Because of the narrowness of the signal and because of the large product branching ratio in this mode, the feed-down is most prominent in this figure.

The lower (green) of the two histograms superimposed on fig. 1a) shows the mass difference distribution obtained when the D^0 candidates were selected from the D^0 mass sideband region. Neither the direct nor the feed-down signal is seen in this background sample. The histogram is normalized so that it is a direct measurement of the amount of combinatorial background from false D^0 candidates. The kaon particle ID cuts are strong enough that most of the kaon candidates are, in fact, really kaons. Therefore about half of the background comes from combinations of real D^0 mesons with real K^+ mesons. This makes it difficult to significantly reduce the background without cutting unacceptably into the signal efficiency. The upper (red) of the two histograms shows the background estimate coming from wrong charge D^0K^- combinations. No signal is seen in this background sample. There is no simple interpretation of the normalization of this background since kaons from the other charmed particle in the event sometimes are swept into the primary vertex. Therefore the sources of right sign and wrong sign kaons have different abundances.

One expects that there might also be a feed-down peak from the process, $D^*_{s2} \rightarrow D^{*0}K^+$, followed by $D^{*0} \rightarrow D^0\pi^0$ or $D^{*0} \rightarrow D^0\gamma$. The magnitude of the expected peak is unknown because there, as yet, exist only upper limits on the ratio of branching fractions, $\mathcal{B}(D^*_{s2} \rightarrow D^*K)/\mathcal{B}(D^*_{s2} \rightarrow DK)$. This peak should appear near a mass difference of 0.56 GeV$/c^2$ and it should have the same width as the $D_{s2} \rightarrow D^0K^+$ peak. There is no evidence for such as peak but in fig. 1a) but such a peak has been allowed for when the spectrum was fitted.

Until now, the decay mode $D_{s2} \rightarrow D^+K^0_S$ has not been observed. To search for this decay mode, the following decay chain was used, $D_{s2} \rightarrow D^+K^0_S$, followed by $D^+ \rightarrow K^-\pi^+\pi^+$ and $K^0_S \rightarrow \pi^+\pi^-$. The D^+ candidates were reconstructed using the candidate driven approach described in section 2. To search for K^0_S candidates, oppositely charged pairs of tracks were considered provided they formed a good vertex and provided the invariant mass of the pair was close to the PDG K^0_S mass. Most of the K^0_S's live long enough that they decay downstream of the silicon strip detectors. Some of the K^0_S's, however, decay after only a short time and do leave tracks in the microstrip detector. In this case the K^0_S candidates were required to pass vertexing requirements similar to those of the D^+ candidates. They were also required to point back to the main vertex seeded by the D^+. On the other hand, those K^0_S without silicon microstrip information, were constrained to come from the the primary vertex of the event.

Each D^+ candidate in an event was combined with each K^0_S candidate, in the same event, that was consistent with coming from the primary vertex. For each $D^+K^0_S$ combination, the mass difference Δ_{s+} was computed, where,

$$\Delta_{s+} \quad = \quad M((K^-\pi^+\pi^+)K^0_S) - M(K^-\pi^+\pi^+). \tag{2}$$

The distribution of the measured Δ_{s+} is shown as the data points in fig. 1b). The prominent feature near a mass difference of 0.7 GeV$/c^2$ is the first observation of the decay $D^*_{s2} \rightarrow D^+K^0_S$. The feed-down peak from $D_{s1} \rightarrow D^{*+}K^0_S$, followed by $D^{*+} \rightarrow D^+\pi^0$ or $D^{*+} \rightarrow D^+\gamma$, is barely visible near a mass difference of 0.525 GeV$/c^2$. This peak is expected to be much less prominent than the corresponding feed-down peak in fig. 1a). The reason is that the D^{*0} decays 100% of the time to D^0 plus neutrals whereas the D^{*+} decays only about one third of the time to D^+ plus neutrals. There is also expected to be a broad feed-down near 0.56 GeV$/c^2$ from the decay $D^*_{s2} \rightarrow D^{*+}K^0_S$ in which the D^{*+} decays to a D^+ plus neutrals. As for the D^0K^+ analysis, the expected yield of such a signal is unknown. There is no evidence for such a structure in this data but it will be allowed for in the fit. The possible narrow structure near a mass difference of 0.65 GeV$/c^2$ is not robust against cuts.

The green histogram lying below the data points shows the contribution which comes from sidebands of the D^+ or the K^0_S. Both the shape and the normalization of the sideband sample contain information. First, there is no signal for the $D^*_{s2} \rightarrow D^+K^0_S$ in this sample, which improves confidence that the signal is real. Second, it is normalized so that is shows the level of the combinatoric background. To be precise the green histogram was obtained by selecting combinations in which the D^+ candidate is in the signal region but the K^0_S candidate is in the sideband region. To this was added combinations in which the K^0_S candidate is in the signal region but the D^+ candidate is in the

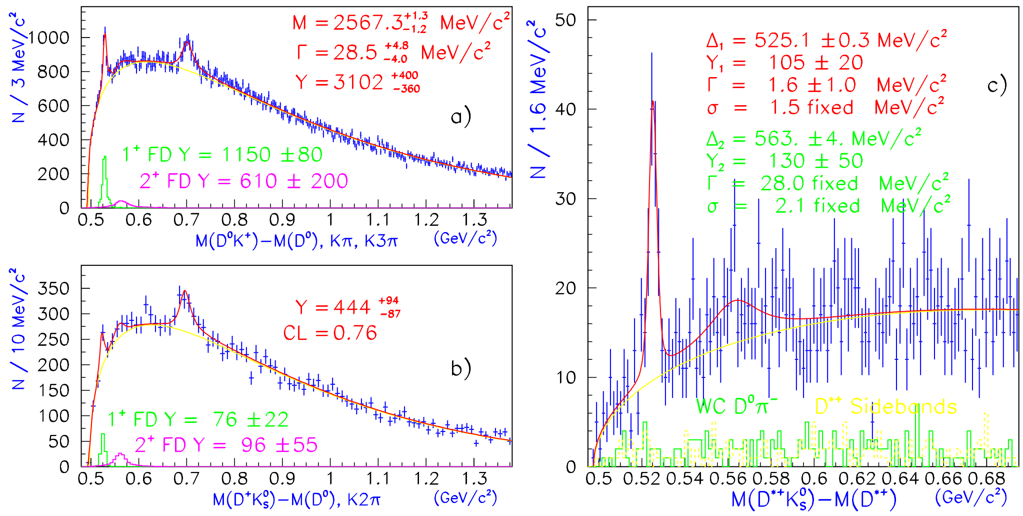

Figure 2: *Mass difference distributions for D^0K^+, $D^+K^0_S$ and $D^{*+}K^0_S$ combinations. The details of the superimposed curves and histograms are described in the text. The errors on the fit parameters are statistical only.*

sideband region. From this sum combinations were subtracted if they fell in the sidebands of both the D^+ and the K^0_S. There are very few entries from both sidebands so the error bars on the histogram entries are only slightly larger than $\sqrt{N}$. One can also see from this plot that just under half of the combinations are combinations of a real D^+ with a real K^0_S; the remainder are combinatoric background. This mode does not have a wrong charge sample which can be used as an independent check of the combinatoric background.

Fig. 2 parts a) and b) shows the same data as in fig. 1 with the addition of superimposed curves which are the result of a combined fit to the two histograms. The fits were performed in two stages. First the two histograms were fitted independently, for which no figure is shown. Then, to obtain the final results, the two histograms were fitted simultaneously and it is the result of this fit which is superimposed on fig.2 parts a) and b). In the independent fits, each histogram was described by a function with four components: the D^*_{s2} signal was parameterized by a D-wave Breit-Wigner; the combinatoric background was parameterized by a smooth function; and the D_{s1} and D^*_{s2} feed-downs were parameterized using a a shape obtained by Monte Carlo (MC) simulation and free normalizations. For the MC simulation, $D^{**}_s \to D^*K$ events were generated using `PYTHIA`, passed through the detector simulation program and passed through the main reconstruction program. The output of this process was analyzed as a DK signal using the same cuts as were applied to the data. This produced Δ_{s0} and Δ_{s+} distributions which were then normalized to unit area and then used to describe the line shapes of the feed-down processes. In summary, the fit to the D^0K^+ data has five interesting free parameters, the mass, width and yield

Table 1: *Results of the fits to the histograms in fig. 2. The errors are statistical only. The columns marked FD refer to the structures which are created by feed-down processes. The top two lines give the results for fitting the D^0K^+ and the $D^+K^0_S$ mass difference spectra separately, while the third and fourth lines give the results for the simultaneous fit to the two spectra; this is the nominal result of the DK analysis.*

Mode	Mass	Width	Yield		
	(MeV/c^2)	(MeV/c^2)	D^*_{s2}	D_{s1} FD	D^*_{s2} FD
D^0K^+	2567.7 ± 1.4	$27.3^{+5.5}_{-4.4}$	3018^{+430}_{-380}	1149 ± 80	595 ± 200
$D^+K^0_S$	$2563.9^{+3.8}_{-3.2}$	$28.^{+11}_{-8}$	450^{+120}_{-110}	76 ± 22	99 ± 55
Combined	2567.3 ± 1.4	$28.5^{+4.8}_{-4.0}$	3102^{+400}_{-360}	1150 ± 80	610 ± 200
			444^{+94}_{-87}	76 ± 22	96 ± 55
			D_{s1}	D^*_{s2}	
$D^{*+}K^0_S$	2535.1 ± 0.3	1.6 ± 1.0	105 ± 20	130 ± 50	

of the D^*_{s2} state, the yield of the D_{s1} feed-down, and the yield of a possible D^*_{s2} feed-down; in addition there are 3 free parameters associated with the smooth background shape. A similar fit function was used to parameterize the $D^+K^0_S$ data. The fit was performed using a binned maximum likelihood fit in bins of 1 MeV/c^2 and in both cases the fit returned an acceptable confidence level. The data was then rebinned, and the fit function rescaled for display purposes.

The results of these fits are summarized in tab. 1. Most importantly the decay mode $D^*_{s2} \to D^+K^0_S$ is observed with a statistical significance of 3.8 standard deviations. In addition, the two decay modes give consistent results for the mass and width of the D^*_{s2}. In neither case is there a significant signal for the feed-down via $D^*_{s2} \to D^{*+}K^0_S$.

One detail of tab. 1 needs additional comment. The FOCUS experiment actually makes a precision measurement, not of the mass of the D_{s2}, but of the mass differences Δ_{s0} and Δ_{s+}. While the mass of the D_{s2} is independent of decay mode, the mass differences differ by the $D^+ - D^0$ mass difference. For ease of comparison among the three mass measurements, tab. 1 reports the mass, not the mass difference. The measured mass differences are 703.2 ± 1.3 MeV/c^2 and $694.6^{+3.8}_{-3.2}$ for the D^0K^+ and $D^+K^0_S$ modes respectively. The numbers reported in tab. 1 are the measured mass differences plus the PDG 2000[6] values of the D masses, $M(D^0) = 1864.5 \pm 0.5$ MeV/c^2 and $M(D^+) = 1869.3 \pm 0.5$ MeV/c^2.

The final results were obtained by a combined fit to the Δ_{s0} and Δ_{s+} distributions. In this fit the mass and width of the D^*_{s2} were fixed to the same value for both isospin substates. All other parameters were kept separate for the two histograms. Therefore there are 8 interesting fit parameters, the mass and width of the D^*_{s2}, the yields of the D^0K^+ and $D^+K^0_S$ signals, and the yields of the four feed-down processes. In addition there are six parameters, 3 per histogram, to describe the smooth background shapes. The results of this fit

Table 2: *Summary of preliminary D_{s2}^* and D_{s1} results. The errors are statistical only. The quoted mass and width were obtained by simultaneous fits to the D^0K^+ and $D^+K_S^0$ mass difference distributions. The PDG[6] values of these quantities are included for comparison.*

State	Mass (MeV/c^2)		Width (MeV/c^2)	
	FOCUS	PDG	FOCUS	PDG
D_{s2}^*	2567.3 ± 1.3	2573.5 ± 1.7	$28.^{+5}_{-4}$	15 ± 5
D_{s1}	2535.1 ± 0.3	2535.35 ± 0.34	1.6 ± 1.0	< 2.3 @ 90% CL.

are summarized in tab. 1. They are consistent with those obtained when the two histograms were fitted independently. The decay mode $D_{s2}^* \to D^+K_S^0$ is now observed with a statistical significance of 4.8 standard deviations.

The other charmed strange meson studied was the D_{s1}, which was reconstructed via the decay chain $D_{s1} \to D^{*+}K_S^0$, followed by $D^{*+} \to D^0\pi^+$, $K_S^0 \to \pi^+\pi^-$, and by $D^0 \to K^-\pi^+$ or $D^0 \to K^-\pi^+\pi^+\pi^-$. For this analysis D^0 and K_S^0 candidates were reconstructed as described earlier. In order to construct D^{*+} candidates, each D^0 candidate in an event was combined with each π^+ candidate, in the same event, that was consistent with coming from the primary vertex. For each $D^0\pi^+$ combination, the mass difference Δ was computed, where

$$\Delta \quad = \quad M((K^-\pi^+[\pi^+\pi^-])\pi^+) - M(K^-\pi^+[\pi^+\pi^-]). \tag{3}$$

Combinations were retained as D^+ candidates if Δ was close to the PDG value of the $D^{*+} - D^0$ mass difference. Each D^{*+} candidate in an event was combined with each K_S^0 candidate, in the same event, that was consistent with coming from the primary vertex. For each $D^{*+}K_S^0$ combination the mass difference Δ_{s+}^* was computed, where,

$$\Delta_{s+}^* = M(D^{*+}K_S^0) - M(D^{*+}). \tag{4}$$

Here D^{*+} should be understood as a shorthand for the measured mass of the candidate. The distribution of Δ_{s+}^* for all candidates which passed the selection cuts is shown as the data points in fig. 2c). The prominent signal at a mass difference near 0.525 GeV/c^2 is the well established D_{s1}. A second signal which may appear in this channel is the decay $D_{s2}^* \to D^{*+}K_S^0$. This would appear near a mass difference of 0.56 GeV/c^2 and would have a width equal to that of the structures observed in the D^0K^+ and $D^+K_S^0$ mass difference spectra, about 28 ± 5 MeV/c^2. There is no clear evidence for such a structure in the data but such a structure has been allowed for in the fit.

The solid (green) histogram below the data points shows the properly normalized contribution from wrong sign combinations, $(D^0\pi^-)K_S^0$ in which the $D^0\pi^-$ system satisfies all of the selection requirements for the D^{*+}. The dashed (yellow) histogram shows the properly normalized contribution from the D^{*+}

sidebands. Neither background sample shows any evidence for either the D_{s1} or the D^*_{s2} resonances. The normalization of the sidebands indicates that the histogram is dominated by combinations of real D^{*+} with real K^0_S, and not by background combinations.

The solid (red) curve superimposed on the data points represents the results of a fit in which the fitting function had the following components: the D_{s1} signal was parameterized by a non-relativistic Breit-Wigner convoluted with a gaussian resolution function; the background was parameterized by a straight line multiplied by a square-root threshold factor; and a possible D^*_{s2} contribution was parameterized by a D-wave Breit-Wigner. In the fit, the σ of the gaussian resolution function was fixed at the value determined by MC studies of the detector resolution, 2.1 MeV/c^2. Also the mass and width of the D^*_{s2} contribution were fixed at the values determined from the DK simultaneous fit. The interesting free parameters in the fit were the mass, width and yield of the D_{s1} signal and the yield of a possible D^*_{s2} signal. In addition there were two free parameters associated with the background function. The fit was performed using a binned maximum likelihood method in bins 0.2 MeV/c^2; after the fit, the data were rebinned and the fit function scaled for display purposes. The results of the fit are summarized in table 1 and the quoted errors are statistical only. The width of the D_{s1} as measured by the fit is consistent with zero but, because the systematic error is not yet determined, no upper limit will be quoted. The fit does not find a significant signal for the decay mode $D^*_{s2} \to D^{*+}K^0_S$.

Tab. 2 gives a summary of the major results from the FOCUS study of P-wave charmed-strange mesons and, for reference, the PDG values of the mass and width of the D^*_{s2} are also given. Before concluding that any discrepancy exists in the D_{s2} data one must remember that the systematic errors for the FOCUS data have yet to be determined. Moreover, the two preceding measurements[7][8] of the D_{s2} were both done at e^+e^- colliders operating at the $\Upsilon(4S)$ and any coherent effects which are present in the production mechanism may well differ between photoproduction and e^+e^- production.

3.2 P-wave Charmed non-strange Mesons

For this study the decay modes used are, $D_2^{*0}(2460) \to D^+\pi^-$ followed by $D^+ \to K^-\pi^+\pi^+$, and $D_2^{*+}(2460) \to D^0\pi^+$ followed by $D^0 \to K^-\pi^+$ or $D^0 \to K^-\pi^+\pi^+\pi^-$. The D^0 and D^+ candidates were reconstructed using the candidate driven approach described in section 2; the combined yield of the two states was about 330,000 with $S/B \simeq 7$. This work is summarized below and more details may be found in ref.[9].

Each D^+ candidate in an event was combined with each π^- candidate in the primary vertex and the mass difference Δ_+ was computed where,

$$\Delta_+ = M((K^-\pi^+\pi^+)\pi^-) - M(K^-\pi^+\pi^+). \tag{5}$$

Fig. 3a) shows the distribution of $\Delta_+ + M_{PDG}(D^+)$, which has two prominent features on top of a smoothly varying background. The peak near 2.46 GeV/c^2

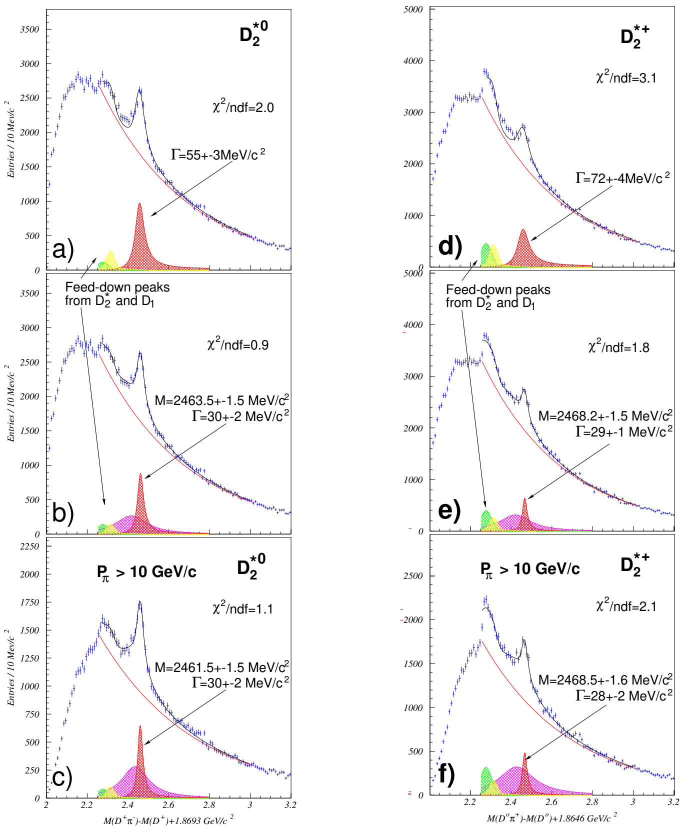

Figure 3: *Invariant mass distributions for $D^+\pi^-$ and $D^0\pi^+$ combinations, as described in the text.*

corresponds to the D_2^{*0}. The structure near 2.3 GeV$/c^2$ arises from two overlapping feed-down structures which are produced by the decays $D_2^{*0} \to D^{*+}\pi^-$ and $D_1^0 \to D^{*+}\pi^-$, followed by $D^{*+} \to D^+\pi^0$ or $D^{*+} \to D^+\gamma$. The distribution was fitted using a function with 3 components: an exponential to parameterize the background shape, a relativistic D-wave Breit-Wigner, convoluted with a gaussian resolution function, to parameterize the D_2^{*0} signal, and a fixed feed-down shape with a free normalization. The σ of the gaussian was fixed at 7 MeV$/c^2$, as determined by a MC simulation of the detector resolution. The slope of the exponential was fixed to that obtained from the mass difference distribution of wrong sign ($D^+\pi^+$) combinations. The shape of the feed-down component was determined by a MC simulation and that shape was include in the fits with a free normalization. The shapes inset at the bottom of the figure show the contributions of the signal and the feed-down to the overall fit. The fit is visibly bad and has a bad χ^2/dof of 2.0.

It is not too surprising that the fit is poor; this distribution should also contain contributions from the predicted broad P-wave states D_0^{*0} and D_1^0, a direct contribution from $D_0^{*0} \to D^+\pi^-$ and a feed-down contribution from $D_1^0 \to D^{*+}\pi^-$. Because the mass splitting between these two states is expected to

Table 3: *Summary of Preliminary D_2^* Results.*

State	Mass (MeV/c^2)		Width (MeV/c^2)	
	FOCUS	PDG[6]	FOCUS	PDG
D_2^{*+}	$2468.2 \pm 1.5 \pm 1.4$	$2459. \pm 4.$	$28.6 \pm 1.3 \pm 3.8$	$25. \pm 8.$
D_2^{*0}	$2463.5 \pm 1.5 \pm 1.5$	2458.9 ± 2.0	$30.5 \pm 1.9 \pm 3.8$	$23. \pm 5.$

be small compared to their width, their contribution can be parameterized by adding one new term to the fit, a relativistic S-wave Breit-Wigner with a free mass, width and normalization. Fig. 3b) shows the same data as fig. 3a) but the superimposed fit includes the extra broad term. The inset at the bottom of this figure now includes the contribution of the broad shape. Visibly this fit is a far superior description of the data and it has good χ^2/dof of 0.9. The mass and width of the broad state are, roughly speaking, within the range predicted by theory. This is not, however, a definitive observation of such a state and the mass and width will not be quoted. The preliminary FOCUS numbers for the properties of the D_2^{*0} come from the fit to this distribution and they are summarized in tab.3; for comparison the corresponding PDG numbers are also included.

The systematic errors quoted in the table come from studies of cut variants. Fig. 3c) shows the results of one such study. The π^- momentum spectrum for true D_2^{*0} decays is rather hard; therefore a requirement of $p_{\pi^-} > 10$ GeV/c improves the S/B. Fig. 3c) shows the experimental data with the minimum momentum cut applied and the overlayed fit contains all of the terms included in the fit to Fig. 3b). The fit has an acceptable χ^2/dof of 1.1 and the results of the fit are consistent with those of the previous fit.

Fig. 3 parts d) through f) show a similar series of fits for the decay $D_2^{*+} \to D^0\pi^+$. Again it is necessary to include a term to allow for the predicted broad states. The preliminary FOCUS numbers for the properties of the D_2^{*+} come from the fit to fig. 3e) and are summarized in tab.3.

4 Σ_c Isospin Mass Splittings

This section discusses the measurement of the isospin mass splittings in the Σ_c system. The first two states considered are the Σ_c^{++} and the Σ_c^0, which were reconstructed using the decays, $\Sigma_c^{++} \to \Lambda_c^+\pi^+$ and $\Sigma_c^0 \to \Lambda_c^+\pi^-$, where $\Lambda_c^+ \to pK^-\pi^+$. The full details of this analysis have already been published[10]. The invariant mass distribution, for all $pK^-\pi^+$ combinations which passed the candidate driven selection are shown in fig. 4. All combinations which fell within 2.1 σ of the nominal Λ_c^+ mass were retained as Λ_c^+ candidates; here σ is the measurement error on the $pK^-\pi^+$ invariant mass, determined separately for each combination. Each Λ_c^+ candidate was combined with each remaining charged pion candidate in the event and the mass difference, $M((pK^-\pi^+)\pi^\pm) -$

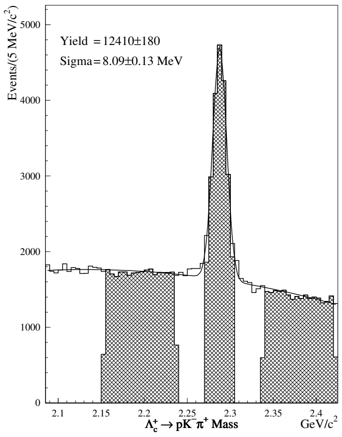

Figure 4: *Invariant mass of* $pK^-\pi^+$ *combinations which survive the candidate driven vertexing. The shaded regions indicate the* Λ_c^+ *signal region and two sideband regions; note that the boundaries of the regions do not coincide with bin boundaries.*

$M(pK^-\pi^+)$ was computed. The mass difference distributions for the two charge states are shown in fig. 5. In each histogram a prominent peak is present near a mass difference of 167 MeV/c^2; these correspond to the Σ_c^0 and. Σ_c^{++}. These distributions were fitted using a smooth function to parameterize the background and a gaussian to parameterize the signal; for this analysis the natural width of the states was ignored. The mass differences determined by the fits are summarized in tab.4. The systematic errors are dominated by the dependence of the result on variations to the analysis cuts; other contributions include the momentum scale of the FOCUS detector, fit variants and reconstruction biases. The precision of the measurement of $M(\Sigma_c^{++}) - M(\Sigma_c^0)$ is similar to that of the PDG average of published results[6]; there is a also new preliminary result by CLEO has slightly better precision[11].

The remaining charmed baryons studies presented here are still preliminary. Additional details about them are available in ref.[12].

The decay mode $\Sigma_c^+ \to \Lambda_c^+\pi^0$ was also investigated. This state has previously been seen by only one experiment[13] and the FOCUS observation represents the first independent confirmation. For this study Λ_c^+ candidates were selected in a fashion similar to that described above, but, in order to obtain a higher yield, the cuts were loosened slightly. Clusters of energy in the inner EM calorimeter were considered as photon candidates and pairs of photons were selected as π^0 candidates if the invariant mass of the pair was within 25 MeV/c^2 of the nominal π^0 mass. For each $(pK^-\pi^+)\pi^0$ combination in an event, the mass difference, $M((pK^-\pi^+)\pi^0) - M(pK^-\pi^+)$, was computed and the distribution of mass differences is shown in fig. 6. The right hand plot was fitted with the same parameterization as the previous two distributions and the results of the fit are summarized in tab.4. The dominant systematic arises from uncertainty

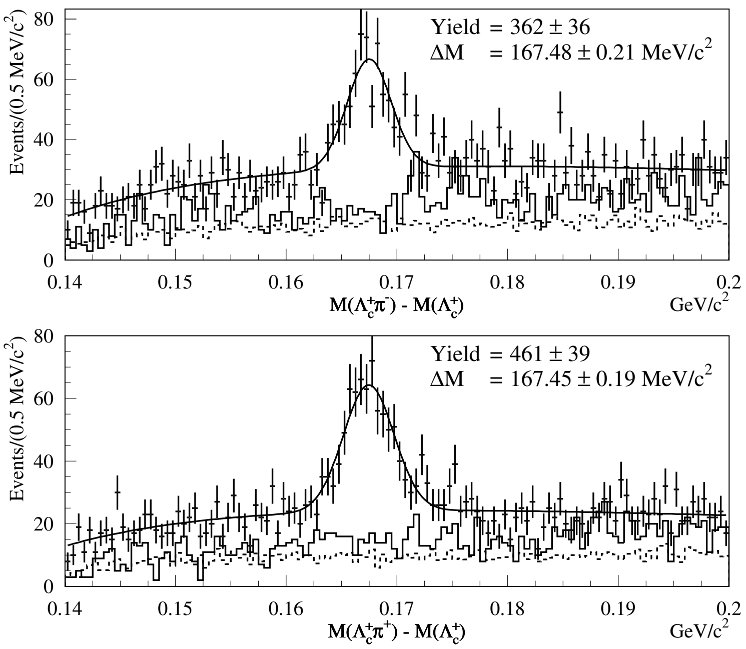

Figure 5: $M((pK^-\pi^+)\pi^\pm) - M(pK^-\pi^+)$ *for combinations passing the requirements discussed in the text. In each plot the data points show the experimental data and the solid curve shows the result of a fit described in the text. The histograms show that no signal is present in two background samples; the solid histogram shows the distribution obtained using* $pK^-\pi^+$ *combinations from the* Λ_c^+ *sideband and the dashed histogram shows the distribution obtained using a* $pK^-\pi^+$ *combination from one event and charged pions from the previous event.*

in the calibration of the geometry of the EM calorimeter.

The decay $\Sigma_c \to \Lambda_c\pi$ is a strong decay and is expected to have a natural width of a few MeV[14]. To measure the natural width of the Σ_c^{++} and the Σ_c^0, $\Lambda_c^+\pi^\pm$ candidates were selected in a fashion similar to that described above. A MC simulation of the detector response showed that the detector resolutions are 2.32 ± 0.23 MeV$/c^2$ for the Σ_c^0 and 2.26 ± 0.24 MeV$/c^2$ for the Σ_c^{++}. The mass difference distributions, similar to those in fig. 5, were fitted using a smooth function to describe the background and a Breit Wigner, convoluted with a gaussian detector resolution, to describe the signal. For the fit the resolution of the gaussian was fixed and the natural width of the Breit-Wigner was allowed to float. The widths obtained from the fit are summarized in tab.4. There are no published measurements for the widths of these states but CLEO Collaboration has presented preliminary results[11].

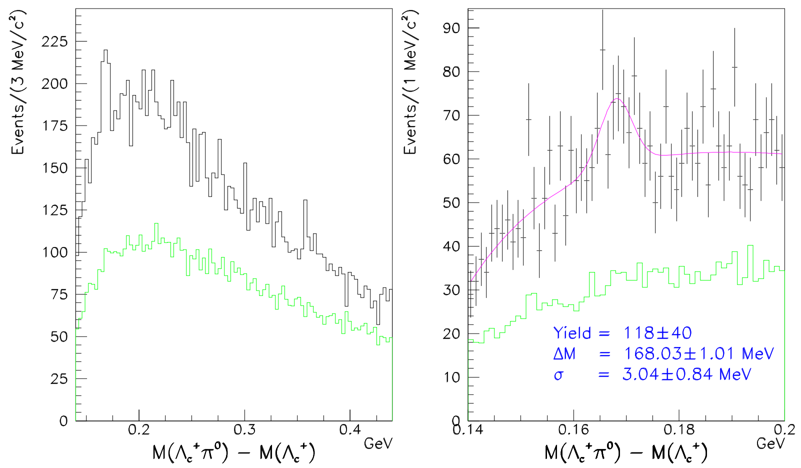

Figure 6: *Mass difference, $M((pK^-\pi^+)\pi^0) - M(pK^-\pi^+)$, for combinations which pass selection criteria described in the text. An enhancement near 168 MeV/c^2 is clearly visible in the left hand plot. The right hand plot shows the same data in a finer binning. In the right figure the data points represent the experimental data, the solid curve is the result of a fit described in the text and the histogram is the distribution obtained using $pK^-\pi^+$ combinations from the Λ_c^+ sidebands.*

5 Observation of the Σ_c^*

FOCUS has preliminary observations of the decays $\Sigma_c^{*++/0} \to \Lambda_c^+\pi^\pm$. These states have previously been seen by only one experiment[11][15] and the FOCUS observation represents the first independent confirmation. This analysis proceeded in a fashion similar to that of the $\Sigma_c^{++/0}$ analyses, with small changes to the details of the Λ_c^+ selection. Fig. 7 shows the mass difference distributions for these modes. The narrow structures near a mass difference of 168 MeV/c^2 are the $\Sigma_c^{++/0}$ states discussed previously and the broad structures near a mass difference of 233 MeV/c^2 are the Σ_c^{++} and Σ_c^0. A MC detector simulation showed that the mass resolution for both Σ_c^* states is 2.8 MeV/c^2. The distributions were fitted using a polynomial to parameterize the background, a gaussian to describe the Σ_c states and a Breit Wigner, convoluted with a gaussian resolution function, to parameterize the Σ_c^* states. The mass differences and widths determined by fit are summarized in tab.4.

6 Conclusions

The FOCUS data contains a wealth of information about charmed hadron spectroscopy. This report presents a preliminary first observation of the decay mode $D_{s2}^* \to D^{*+}K_S^0$. It also presents new, high statistics measurements of the the the masses and widths of five of the six narrow P-wave charmed mesons. FOCUS has presented a measurement of the $\Sigma_c^{++} - \Sigma_c^0$ mass splitting which is compet-

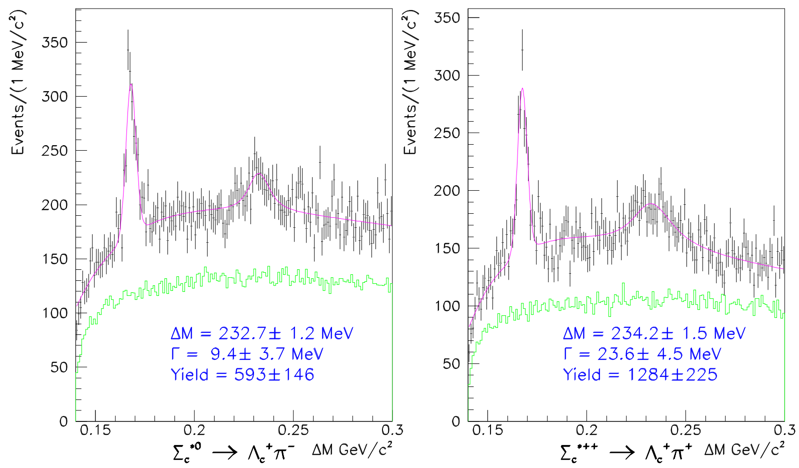

Figure 7: *Mass difference,* $M((pK^-\pi^+)\pi^\pm) - M(pK^-\pi^+)$*, for combinations which pass selection criteria described in the text. The data points are the experimental data, the solid curve is the result of a fit described in the text and the histogram is the estimate of the background from* Λ_c^+ *sidebands.*

Table 4: *Summary of* Σ_c *Measurements. The measurements of the natural widths and all results pertaining to the* Σ_c^+ *or the* Σ_c^* *are preliminary.*

State	$M - M(\Lambda_c^+)$ (MeV/c^2)	Γ (MeV/c^2)	$M - M(\Sigma_c^0)$ (MeV/c^2)
Σ_c^{++}	$167.35 \pm 0.19 \pm 0.12$	$2.53 \pm 0.77^{+0.51}_{-0.56}$	$-0.03 \pm 0.28 \pm 0.11$
Σ_c^{+}	$168.0 \ \ \pm 1. \quad \pm 0.3$	-	$0.6 \ \ \pm 1. \quad \pm 0.3$
Σ_c^{0}	$167.38 \pm 0.21 \pm 0.13$	$2.58 \pm 0.79^{+0.51}_{-0.55}$	-
Σ_c^{*++}	234.2 ± 1.5	23.6 ± 4.5	$M(\Sigma_c^{*0}) - M(\Sigma_c^{*++})$
Σ_c^{*0}	232.7 ± 1.2	9.4 ± 3.7	$= -1.5 \pm 1.9$

itive with the best published measurements. FOCUS confirms the existence of the Σ_c^+, the Σ_c^{*++} and the Σ_c^{*0} and preliminary numbers for their properties have been shown. And a non-zero natural width for the Σ_c is also confirmed at the 3 σ level.

7 Acknowledgements

The author would like the thank the conference organizers for their hospitality and for their hard work to ensure an enjoyable, well run conference. The FOCUS collaborations wishes to acknowledge the assistance of the staffs of Fermi National Accelerator Laboratory, the INFN of Italy, and the physics departments of the collaborating institutions. This research was supported in part by the U. S. National Science Foundation, the U. S. Department of Energy, the Italian Istituto Nazionale di Fisica Nucleare and Ministero dell'Università e della Ricerca Scientifica e Tecnologica, the Brazilian Conselho Nacional de Desenvolvimento Científico e Tecnológico, CONACyT-México, the Korean Ministry of Education, and the Korean Science and Engineering Foundation.

8 References

References

[1] The members of the FOCUS collaboration are coauthors of this paper: J.M. Link, V.S. Paolone, M. Reyes, P.M. Yager (**UC DAVIS**); J.C. Anjos, I. Bediaga, C. Göbel, J. Magnin, J.M. de Miranda, I.M. Pepe, A.C. dos Reis, F.R.A. Simão (**CPBF, Rio de Janeiro**); S. Carrillo, E. Casimiro, H. Mendez, A.Sánchez-Hernández,, C. Uribe, F. Vasquez (**CINVESTAV, México City**); L. Cinquini, J.P. Cumalat, J.E. Ramirez, B. O'Reilly, E.W. Vaandering (**CU Boulder**); J.N. Butler, H.W.K. Cheung, I. Gaines, P.H. Garbincius, L.A. Garren, E. Gottschalk, S.A. Gourlay, P.H. Kasper, A.E. Kreymer, R. Kutschke (**Fermilab**); S. Bianco, F.L. Fabbri, S. Sarwar, A. Zallo (**INFN Frascati**); C. Cawlfield, D.Y. Kim, K.S. Park, A. Rahimi, J. Wiss (**UI Champaign**); R. Gardner (**Indiana**); Y.S. Chung, J.S. Kang, B.R. Ko, J.W. Kwak, K.B. Lee, S.S. Myung, H. Park (**Korea University, Seoul**); G. Alimonti, M. Boschini, D. Brambilla, B. Caccianiga, A. Calandrino, P. D'Angelo, M. DiCorato, P. Dini, M. Giammarchi, P. Inzani, F. Leveraro, S. Malvezzi, D. Menasce, M. Mezzadri, L. Milazzo, L. Moroni, D. Pedrini, F. Prelz, M. Rovere, A. Sala, S. Sala (**INFN and Milano**); T.F. Davenport III (**UNC Asheville**); V. Arena, G. Boca, G. Bonomi, G. Gianini, G. Liguori, M. Merlo, D. Pantea, S.P. Ratti, C. Riccardi, P. Torre, L. Viola, P. Vitulo (**INFN and Pavia**); H. Hernandez, A.M. Lopez, L. Mendez, A. Mirles, E. Montiel, D. Olaya, J. Quinones, C. Rivera, Y. Zhang (**Mayaguez, Puerto Rico**); N. Copty, M. Purohit, J.R. Wilson (**USC Columbia**); K. Cho, T. Handler (**UT Knoxville**); D. Engh, W.E. Johns, M. Hosack, M.S. Nehring, M. Sales, P.D. Sheldon, K. Stenson, M.S. Webster (**Vanderbilt**); M. Sheaff (**Wisconsin, Madison**); Y. Kwon (**Yonsei University, Korea**).

[2] Information about the FOCUS detector and FOCUS physics results are available at the URL, http://www-focus.fnal.gov.

[3] P.L. Frabetti *et al* (E687 Collab.), Nucl. Instrum. Methods A **320**, 519 (1992).

[4] J.M. Link et al. (FOCUS Collab.), Phys. Lett. **B485** 62 (2000).

[5] J. Bartelt and S. Shukla, Ann. Rev. Nucl. Part. Sci. **45** 83 (1995).

[6] D.E. Groom *et al*, European Phys. Jour. C, **15** 1 (2000).

[7] Y. Kubota et al. (CLEO Collab.), Phys. Rev. Lett. **72** 1972 (1994).

[8] H. Albrecht et al. (ARGUS Collab.), Zeit. Phys. **C69** 405 (1994).

[9] S. Sarwar *et al.* (FOCUS Collab.), "Preliminary results on charmed meson spectroscopy," hep-ex/0011072.

[10] J.M. Link et al. (FOCUS Collab.), Phys. Lett. **B488** 218 (2000).

[11] A. Warburton, Talk presented at ICHEP2000 hep-ex/0009040, (2000).

[12] E.W. Vaandering, Ph.D Thesis, University of Colorado (Boulder), (2000) unpublished. A copy of the thesis is available from ref.[2].

[13] R. Ammar, *et al*, (CLEO Collab.) hep-ex/0007041, CLEO 00-13 (2000). Submitted for publication.

[14] See citations in ref.[12].

[15] G. Brandenburg *et al*, (CLEO Collab.) Phys. Rev. Lett. **78** 2304 (1997).